Anisotropy of *c* facets of ⁴He crystal

I. A. Todoshchenko,[1] M. S. Manninen,[1] and A. Ya. Parshin[2]

[1]*Low Temperature Laboratory, Aalto University, P.O. Box 15100, FIN-00076 Aalto, Finland*

[2]*P. L. Kapitza Institute, RAS, Kosygina 2, Moscow 119334, Russia and Moscow Institute of Physics and Technology, Institutskiy 9, Dolgoprudny 141700, Russia*

Recently, we have observed the so-called devil's staircase of high-order facets on the surface of hcp ⁴He crystals at 0.2 K. Such high roughening temperatures of high-order facets belonging to the $[10\bar{1}N]$ family suggest that there must be an anomaly in the stiffness of vicinal surfaces and of the step on the basal *c* facet at the corresponding orientation. We were able to measure the stiffness of the step on the [0001] *c* facet and the azimuthal stiffness of vicinal surfaces at small polar angles. We have found a strong anisotropy of the stiffnesses at low temperatures, as high as 5–10. The anisotropy rapidly decreases as temperature increases and saturates at low temperatures, in good agreement with the theory of renormalization by thermal fluctuations of the surface. The observed anomaly in the surface stiffness can explain the presence of high-order facets.

Helium crystal is a perfect model system to study the general properties of crystalline matter and surfaces. Due to its essentially quantum nature, helium is the only substance whose liquid-solid interface can be cooled down to low temperatures where the heat and mass diffusion in the bulk phases is very fast and the interface manifests its intrinsic properties. Faceting, i.e., the presence of flat faces, is the most exciting phenomenon taking place on the crystal surface, and according to the theoretical predictions,[1] classical crystals must show an infinite number of facets at zero temperature, where thermal fluctuations of the surface are absent. Quantum fluctuations of the interface do not destroy facets but decrease the free energy of the elementary step.[2–4]

In our recent work we have been searching for new facets on the surfaces of hcp ⁴He crystals at temperatures down to 10 mK.[5] We have used the method of a directional histogram and detected large, flat faces corresponding to high-order facets of $[10\bar{1}N]$ type. Such a devil's staircase of facets has been observed earlier only on the surface of liquid crystals,[6,7] which are extremely soft water solutions of surfactant molecules rather than usual crystals. A devil's staircase on ⁴He crystal surface was not observed before because the free energy of an elementary step on a high-order facet is small and facets are very unstable and can be observed only very close to equilibrium. We were able to prepare crystal surfaces in quasiequilibrium conditions, with a deviation from the equilibrium melting pressure as small as 1–10 μbar, and the sizes of the observed high-order facets were up to 1 mm.

These high-order facets have been seen on ⁴He crystals at temperatures much higher than the temperatures of their roughening transitions predicted by the universal relation

$$T_R = \frac{2}{\pi}\sqrt{\gamma_{||}\gamma_{\perp}}d^2, \qquad (1)$$

where d is the lattice period in the direction perpendicular to the facet. The principal components of the surface stiffness tensor $\hat{\gamma}$, $\gamma_{||} = \alpha + \alpha''_{\theta\theta}$ and $\gamma_{\perp} = \alpha + (1/\sin^2\theta)\alpha''_{\phi\phi} + \cot\theta\,\alpha'_{\theta}$ (α is the surface tension), have been measured to be in the range 0.15–0.2 erg/cm²[8–10] for orientations that are not very close to the basic [0001]*c* facets and $[10\bar{1}0]a$ facets. The universal

relation (1) gives thus 60 mK for the roughening transition temperature of the $[10\bar{1}9]$ facet, which we have observed at 140 mK in experiment.

The discrepancy between the theory and our observations could be explained by the anomalously high surface stiffness in the directions corresponding to the high-order facets of $[10\bar{1}N]$ type. Indeed, a crystal lattice induces natural anisotropy in the stiffness of nondisturbed surfaces, but surface fluctuations blur it out, which might be the reason that Andreeva and Keshishev did not observe the azimuthal anisotropy of the stiffness at 0.4 K.[9] Thus there is a question whether the anisotropy is present at lower temperatures where surface oscillations are much weaker. Such an anisotropy would result in the anisotropy of the elementary step on the basal *c* facet, so that the equilibrium shape of the facet would be noncircular.

In this paper we report our recent measurements of the equilibrium shapes of the basic *c* facet and of the vicinal surfaces of hcp ⁴He crystals in the range 10–400 mK. At low temperatures we have observed a strong (up to a factor of 6) anisotropy of the stiffness of a step on the basal *c* facet and of the perpendicular component of the surface stiffness. We show that the observed temperature dependence of the stiffness agrees well with the fluctuation renormalization theory.

In our experiments we observed the surface of ⁴He crystals with a low-temperature Fabry-Pérot interferometer[11] made of two semitransparent windows thermally anchored to the mixing chamber. Light passed the experimental cell through fused silica windows, and the interference pattern was formed on a cold charge-coupled device (CCD) camera placed inside the vacuum can. The phase shift of the interfering light is proportional to the thickness of the crystal, and thus the true three-dimensional (3D) shape of the crystal could be reconstructed from the interferogram. In order to observe crystals very close to equilibrium conditions we have used a cryogenic valve that allowed us to set liquid helium flow to or from the cell as low as 10^{-12} cm³/s.

We have started our search for anisotropy of the step on the basal *c* facet by measuring the equilibrium shapes of

this facet. In the absence of gravity, the equilibrium shape of a facet obeys the two-dimensional analog of Wulff's theorem: $R(\phi) \propto \beta(\phi)$, where R is the distance from the tangent of the facet contour to the origin. We were able to grow a very good quality crystal with the c facet tilted by $\delta = 2°$ with respect to horizon. Such a small angle makes the contribution of gravity negligible because the variation of the gravitational pressure over a facet of a few millimeters size L is $\rho_L g L \delta \sim 1 \ \mu$bar, while the Laplace pressure due to curvature of the step $\beta \rho_L / d L \Delta \rho$ ($\beta = 4 \times 10^{-10}$ erg/cm[10]) is several tens of microbars. As steps are very mobile, the edge step is always in local equilibrium so that the Laplace pressure exactly compensates the overpressure in liquid and is thus constant over the edge step even if the size of a facet is far from the equilibrium one. Neglecting gravity and assuming anisotropy of the step, the equilibrium condition for the contour of the facet can be written as $\tilde{\beta}(\phi)C = $ const where $\tilde{\beta} \equiv \beta + \beta''_{\phi\phi}$ is the step stiffness and C is the local curvature of the step.

The most fruitful and direct method to measure the shape of the facet was to observe the facet at rest. Usually, a facet grows due to screw dislocations, which terminate on a facet, providing loops of the steps. If the overpressure $\delta p = p - p_{eq}$ is high enough so that the critical size of the terrace $R_c = \beta/(d\delta p)(\rho_L/\Delta\rho)$ is smaller than the distance between dislocations, the loops reconnect, forming growing terraces of a new layer. At low overpressures, however, the curvature of the loops is too small for reconnection, and the facet is absolutely immobile. In contrast, the rough surface that surrounds the facet grows without thresholds and thus can be distinguished unambiguously from the facet. In our measurements we took two consequent interferograms of slowly growing or melting crystal [see an example of a single interferogram in Fig. 1(a)] and calculated the difference between two images. The area corresponding to the immobile facet has a very low intensity on the difference image because the interference fringes did not move during the time between the two interferograms, while areas corresponding to moving
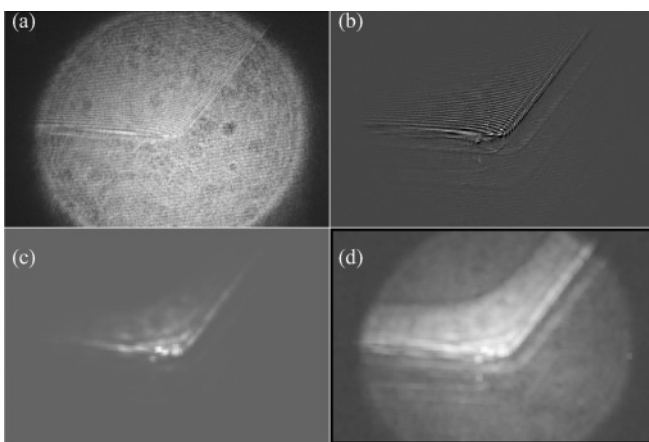

FIG. 1. Finding the shape of the immobile facet: (a) original interferogram of slowly growing crystal (575×383 pixels, 4-mm radius of optical area), (b) difference between two consecutive interferograms, (c) contrast of the difference image, and (d) 1/4 power of the intensity of the contrast image. See text for details.
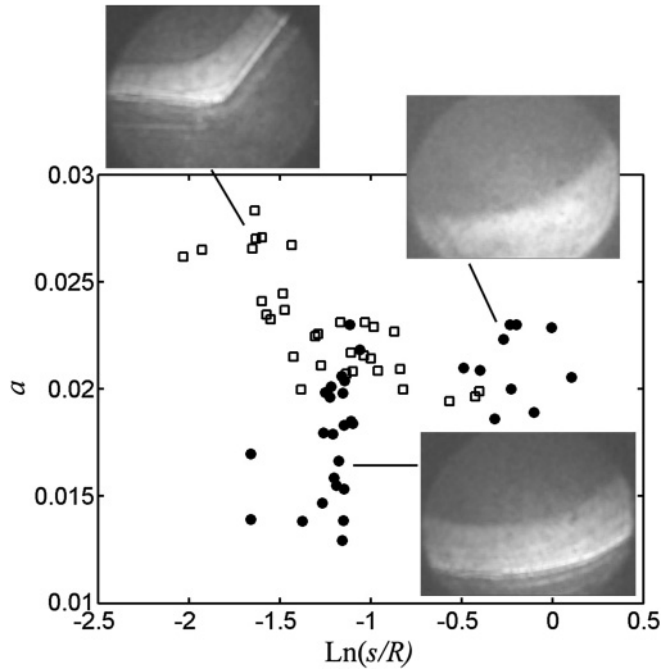
rough surfaces contain fringes after subtracting [Fig. 1(b)]. The next step was to calculate the contrast of the difference image from 10×10 pixel area near each pixel. The contrast of the area representing the facet is very small in comparison to high-contrast areas near the crystal edges [Fig. 1(c)], and the facet can hardly be found by an eye directly. To lift up the intensity of the dark areas we took a small power (1/4 or 1/8) from the contrast image, which made areas of lowest contrast evident [Fig. 1(d)]. In the final image it is clearly seen that the contrast of the facet is as low as the contrast of the solid-free region where definitely no motion of interference fringes occurred. Thus the dark region with the very sharp boundary in the top left part of the image corresponds to an immobile facet. The observed shapes of the c facet were, indeed, far from circular and had corners in the directions between two a facets.

The relation $\tilde{\beta}(\phi)C = $ const for the edge step is valid if the local overpressure is the only force acting on the step. In fact, one should consider also an interaction between the "last" edge step and other steps surrounding the facet. A vicinal surface, i.e., a surface tilted by a small angle with respect to a facet, consists of atomically flat terraces that have the same orientation as the facet has and elementary steps that separate them. The density of steps increases with the tilting angle, and at angles $\sim5°$,[12] the steps start to overlap, and the surface becomes uniformly rough until the orientation of another facet is reached. This means that the equilibrium shape of the rough surface surrounding the basal c facet is affected by the presence of other facets on the crystal surface, and the anisotropy of the c facet [Fig. 1(d)] could be enhanced by the presence of large vertical a facets on the crystal edges.

The influence of the shape of the crystal edge on the shape of the top c facet becomes smaller when the distance s between the edge of the facet and the edge of the crystal increases. In order to eliminate this influence we have measured the shape of the c facet in rather wide range of distances s on growing and melting crystals of different sizes and shapes. In contrast to a growing crystal, a crystal that was melted for some time has the symmetrical rounded shape, as shown in the bottom inset of Fig. 2. The anisotropy of the top c facet is, indeed, somewhat smaller than in the case of growing crystal (left inset of Fig. 2) but is still evident. To avoid any influence of the free crystal edges we have measured also crystals that filled completely the bottom of the cell so that the crystal edge coincided with the cylindrical cell wall. In this case the shape of the top facet is also anisotropic (top right inset of Fig. 2), which proves the anisotropy of the step energy on the basal c facet. The observed contours of the c facets were fitted with the simplest possible function of sixfold symmetry $R = R_0(1 - a \cos 6\phi)$. The dependence of the anisotropy coefficient a on the distance s between the facet and crystal edges at $T = 0.14$ K is shown in Fig. 2.

Indeed, the anisotropy coefficient a depends significantly on the distance to the crystal edge at small s, where the shape of the facet rather mimics the shape of the edge than shows its intrinsic anisotropy. However, when the distance s is relatively large compared to the facet size R, the anisotropy coefficient saturates at the level of $a = 0.021 \pm 0.002$. Because of the sixfold symmetry the measured anisotropy is rather high

FIG. 2. Anisotropy coefficient a of the contour of the c facet as a function of relative distance s/R from the facet to the edge of the crystal. Open squares: growing crystals with large a facets on the crystal edge (top left inset); the anisotropy of the top c facet is enhanced. Solid circles: melting crystals with a symmetric circular free edge (bottom inset) and with an edge touching the cylindrical cell wall (top right inset); the anisotropy of the top c facet is diminished. $T = 140$ mK.

despite the value of a being much smaller than unity. Indeed, the requirement of convexity $R^2 + 2R_\phi'^2 - RR_{\phi\phi}'' > 0$ of the contour described by the form $R = R_0(1 - a \cos 6\phi)$ sets the maximum possible value of about $1/35$ for the anisotropy coefficient a. The stiffness of the step $\tilde\beta$ is inversely proportional to the local curvature of the contour, which varies as $C = (1/R_0)(1 - 35a\cos 6\phi)$ (terms of order a^2 ignored). With the measured value of the anisotropy coefficient a the step stiffness $\tilde\beta = \beta_0/(1 - 35a\cos 6\phi)$ has very strong anisotropy $\tilde\beta_{max}/\tilde\beta_{min} = 6$.

In order to understand the observed results we have adopted the standard theory of renormalization by thermal fluctuations of the surface in the weak-coupling approximation.[13] The simplest Hamiltonian that accounts for the symmetry of the crystal lattice is

$$E(z(\mathbf{r})) = \int\int d^2r \left[\frac{1}{2}\gamma(\nabla z)^2 - V\cos\frac{2\pi z}{d} \right. $$
$$\left. + \varepsilon\gamma|\nabla z|^3\cos 3\phi\sin\frac{\pi z}{d} \right]. \quad (2)$$

The first two terms represent the usual sine-Gordon Hamiltonian: additional surface energy due to gradients and pinning potential $-V\cos\frac{2\pi z}{d}$ induced by the lattice, which acts to keep the surface at the atomic plane position. The last term represents the anisotropy with respect to the azimuthal angle ϕ of the gradient ∇z. Note that the anisotropy term changes sign when the surface moves one atomic plane up. The shape and

the free energy of the elementary step are found by the minimization of the Hamiltonian (2), in which the values of pinning amplitude V, stiffness γ, and anisotropy ε are renormalized by the short-scale thermal fluctuations. During the renormalization procedure we start from the natural, "bare" values V_0, γ_0, and ε_0, which correspond to the nonfluctuating surface and consistently take into account free thermal fluctuations of the surface in the range from k to $k - dk$, starting from the highest possible wave vector $k_0 = \pi/d$. We have restricted the consideration to the first-order approximation, which is reasonable in the case of weak coupling ($V \ll \gamma$) at temperatures much lower than the c facet roughening transition temperature, 1.3 K (the weakness of the coupling is due to quantum fluctuations of the surface). In this approximation the surface stiffness is not renormalized, while the renormalization of the pinning amplitude is $dU/dl = U[2 - \pi T/(\gamma d^2)]$ and that of the anisotropy is $d\varepsilon/dl = dU/4dl$, where $U = V/k^2$ and $l = \log k_0/k$. The renormalization stops at a certain wave vector k_* when the renormalized pinning energy $U(k_*)$ reaches temperature and thus stabilizes the surface at larger scales. The renormalized values of the pinning amplitude $V(k_*)$ and of the anisotropy $\varepsilon(k_*)$ are those that the surface shows at all scales $> 1/k_*$.

The minimization of the Hamiltonian (2) gives the universal shape of the step, which, with accuracy up to ε^2, is

$$Z(X) = 4\arctan e^X - 8\varepsilon'\sinh X/\cosh^2 X$$
$$+ 16\varepsilon'^2[\sinh X/\cosh^2 X + 4\sinh X/\cosh^4 X],$$

where the dimensionless coordinate and height are $X = 2\pi x\sqrt{V/\gamma}/d$, $Z = 2\pi z/d$, and $\varepsilon' = \cos 3\phi\sqrt{V/\gamma}\varepsilon$. The free energy of the step has thus threefold symmetry:

$$\beta = 4d/\pi\sqrt{V\gamma}[1 \pm 4/3\varepsilon\cos 3\phi\sqrt{V/\gamma}$$
$$- (64/15)\varepsilon^2\cos^2 3\phi V/\gamma + o(\varepsilon^2)].$$

However, in macroscopic measurements it is impossible to distinguish neighboring steps, and we observe the value equal to the semisum of their energies, which has sixfold symmetry:

$$\beta = (4d/\pi)\sqrt{V\gamma}[1 - (32/15)(V/\gamma)\varepsilon^2\cos 6\phi + o(\varepsilon^2)]. \quad (3)$$

The accuracy of our measurements on the facet contour is not enough to verify the temperature and angular dependence of the step stiffness. Fortunately, there are other means to measure the step stiffness by using the interferometric images of vicinal surfaces. The surface tilted by a small angle θ with respect to the basal facet can be viewed as a set of the steps of the basal facet with density $n = \theta$. The stiffness of such a surface is determined by the properties of the step. The parallel component of the stiffness is due to the repulsion between steps, $\varepsilon_{s-s} = \delta/l^2$ (l is the distance between steps), which resists against increasing density of steps,

$$\gamma_\parallel = 6\delta\theta/d^3. \quad (4)$$

The perpendicular component of the stiffness is due to the resistance of individual steps against bending,

$$\gamma_\perp = \tilde\beta/d\theta. \quad (5)$$

Both components of the surface stiffness have very strong polar (with respect to θ) anisotropy, which was measured by Andreeva and Keshishev[9] and Rolley et al.,[10] but no azimuthal

(with respect to angle ϕ) anisotropy was ever observed. Actually, Andreeva and Keshishev measured only the parallel component $\gamma_\parallel$, which is isotropic with respect to azimuthal angle ϕ because the rotation does not change the distance and interaction between steps. Rolley *et al.* measured also the perpendicular component but only in one direction, assuming that there is no dependence on ϕ.

We have made measurements on the perpendicular component $\gamma_\perp$ of the stiffness of the vicinal surface as a function of the azimuthal angle ϕ at temperatures 12, 140, and 380 mK by measuring simultaneously both principal components of the curvature of the surface. The Laplace equation for surface pressure and the equilibrium condition for chemical potentials $\mu_L = \mu_S$ connect the local curvature components and the corresponding components of the stiffness with the overpressure in liquid $\gamma_1 C_1 + \gamma_2 C_2 = \delta p(\rho_S - \rho_L)/\rho_L$. For measurements of curvature we chose an area on interferogram around a certain point and fitted the interference phase, which is proportional to the crystal height, with the second-order polynomial of the spatial coordinates. The curvatures $C_\parallel$ (in the θ plane) and $C_\perp$ (in the plane perpendicular to the θ plane) were obtained from the fit together with the local height h of the surface. The perpendicular component of the surface stiffness was calculated as $\gamma_\perp = (1/C_\perp)\{-\gamma_\parallel C_\parallel - \Delta\rho g(h - h_0)\}$. The values of $\gamma_\parallel$ were taken from measurements by Rolley *et al.*,[10] and the unknown reference height h_0 for each interferogram was chosen so that $\gamma_\perp$ was symmetric with respect to $\phi = 0$. All measurements of the stiffness have been done with slowly melting crystals so that no (or very small) high-order facets were present on the analyzed surfaces.

The results of the measurements on the perpendicular component of vicinal surface stiffness is presented in Fig. 3. The scatter of the original data was rather high, and it was difficult to establish certain dependence of the stiffness on angle θ. To reduce the scatter we have averaged stiffnesses measured for surfaces with the polar angle θ in the range from $2°$ to $4°$ (average value of θ is $2.9°$). As one can see, the anisotropy of perpendicular stiffness is rather high at low temperatures. The ratio of the maximum value to minimum value is about 5, which agrees well with the measured anisotropy of the elementary step stiffness $\tilde{\beta}$ measured from the facet contour. The temperature dependence of the stiffness is consistent with the renormalization theory shown by the solid curves with the values $V_0 = 2.6 \times 10^{-3}$ erg/cm^2 and $\varepsilon_0 = 0.75$. The stiffness of the elementary step corresponding to the measured value of the surface stiffness is $\tilde{\beta} = \gamma_\perp d\theta$ and reaches 2.4×10^{-9} erg/cm at low temperatures and small ϕ. The reported earlier[10] value $\beta = 4 \times 10^{-10}$ erg/cm is comparable to the minimum of the value $\gamma_\perp d\theta$ at $\phi = 20°$–$30°$.

We should mention, however, that our analysis of the experimental data is only valid at low temperatures because at $T \gtrsim 0.1$ K the entropic interaction between steps becomes stronger than the elastic one, and the parallel component of the stiffness is no longer isotropic but depends on the step stiffness.[12] Nevertheless, the typical parallel Laplace term, $\gamma_\parallel C_\parallel$, had, in our measurements, a value of about 1/3 the hydrostatic term $\Delta\rho g(h - h_0)$ at 140 mK and about 1/4 of it at 380 mK, which means that the possible error coming from the anisotropy of the parallel stiffness is less than 20%.
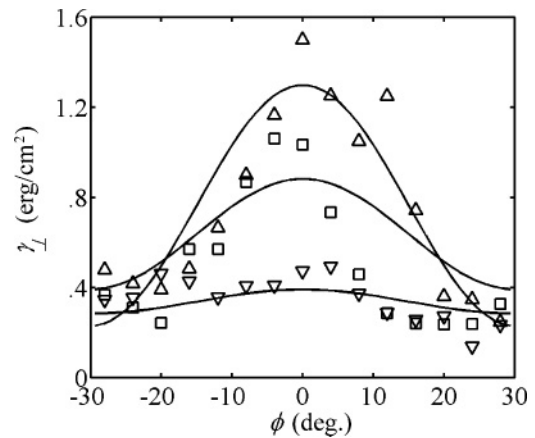

FIG. 3. Perpendicular component of the stiffness of the vicinal ($\theta = 2°$–$4°$) surface of a ^{4}He crystal at temperatures of 12 mK (upward triangles), 140 mK (squares), and 380 mK (downward triangles). Solid curves are the fit with $\gamma_\perp = \tilde{\beta}(T)/(d\bar{\theta})$, where $\beta(T)$ is found from Eq. (3) and the renormalization procedure with $V_0 = 2.6 \times 10^{-3}$ erg/cm^2 and $\varepsilon_0 = 0.75$ (see text).

The observed anomaly in the stiffness of vicinal surfaces explains the relatively high roughening temperatures of high-order facets. The distance between atomic planes of type $[IJ\overline{I+J}N]$ can be found as $d_{IJ\overline{I+J}N} = 6d/\sqrt{32(I^2 + J^2 + IJ) + 9N^2}$. The universal relation(1) contains the product of the surface stiffness components, Eqs. (5) and (4), which turns out to be the product of the step stiffness and step-step interaction, $\gamma_\parallel\gamma_\perp = 6\delta\tilde{\beta}/d^4$. If we use the value of the step-step interaction measured by Rolley *et al.* at 0.1 K, $\delta = 1.4 \times 10^{-23}$ erg cm, and measured here step stiffness at $\phi = 0$, $\tilde{\beta} = 2 \times 10^{-9}$ erg/cm, we find $T_{R,[10\overline{1}N]} = (2/\pi)\sqrt{6\delta\tilde{\beta}}(d_{IJ\overline{I+J}N}/d)^2 \approx 8$ K/N^2, or 100 mK for the $[10\overline{1}9]$ facet. In fact, we have observed facets with even larger Miller indices, which probably means that the maximum of the stiffness is sharper than $\cos 6\phi$ and the value of the stiffness at $\phi = 0$ is even larger than in Fig. 3 but was averaged out because of the large fitting windows. In the view of such a possibility it is important to measure the azimuthal anisotropy of the stiffness by more accurate methods, for instance, by crystallization waves.

To summarize, we have measured the anisotropy of the step on the basal c facet and of vicinal surfaces of ^{4}He crystals. Below 200 mK the anisotropy of the stiffnesses is as high as 5, and the temperature dependence of the stiffness is in a reasonable agreement with fluctuation renormalization theory. We show that the observed anomaly can explain the relatively high roughening temperatures for high-order facets observed in our recent work.[5]

[1] L. D. Landau, *Collected Papers* (Pergamon, Oxford, 1971).

[2] D. S. Fisher and J. D. Weeks, Phys. Rev. Lett. **50**, 1077 (1983).

[3] S. V. Iordanskiĭ and S. E. Korshunov, Sov. Phys. JETP **60**, 528 (1984).

[4] I. A. Todoshchenko, H. Alles, H. J. Junes, A. Ya. Parshin, and V. Tsepelin, Phys. Rev. Lett. **93**, 175301 (2004).

[5] I. A. Todoshchenko, H. Alles, H. J. Junes, M. S. Manninen, and A. Ya. Parshin, Phys. Rev. Lett. **101**, 255302 (2008).

[6] P. Pieranski, P. Sotta, D. Rohe, and M. Imperor, Phys. Rev. Lett. **84**, 2409 (2000).

[7] P. Nozières, F. Pistolesi, and S. Balibar, Eur. Phys. J. B **24**, 387 (2001).

[8] P. E. Wolf, F. Gallet, S. Balibar, E. Rolley, and P. Nozières, J. Phys. **46**, 1987 (1985).

[9] O. A. Andreeva and K. O. Keshishev, Phys. Scr. T **39**, 352 (1991).

[10] E. Rolley, C. Guthmann, E. Chevalier, and S. Balibar, J. Low Temp. Phys. **99**, 851 (1995).

[11] V. Tsepelin, H. Alles, A. Babkin, R. Jochemsen, A. Ya. Parshin, and I. A. Todoshchenko, J. Low Temp. Phys. **129**, 489 (2002).

[12] S. Balibar, H. Alles, and A. Ya. Parshin, Rev. Mod. Phys. **77**, 317 (2005).

[13] P. Nozières and F. Gallet, J. Phys. (Paris) **48**, 353 (1987).